Combustion of Carbon Particles in a Hypersonic Turbulent Boundary Layer

A. T. WASSEL* AND A. F. MILLS†
Science Applications, Inc., El Segundo, Calif.

Combustion of carbon ejecta particles in a hypersonic turbulent boundary layer on a missile aft-heat shield is analyzed. A Couette flow model is used and the coupled momentum, mass species, and energy equations are solved by a finite difference technique. Numerical results are obtained for conditions typical of reentry through an erosive environment. The Reynolds analogy factor based on heat flux into the heat shield is shown to be practically independent of particle size and distribution across the boundary layer, i.e., is unaffected by ejecta combustion. The heat flux itself is also unaffected when the particles are distributed close to the wall, but is reduced as a result of variable density effects when the particles are distributed across the boundary layer. It is concluded that because of oxygen depletion in the boundary layer, the over-all effect of carbon ejecta combustion on aft reentry vehicle heat shield transfer rates is small.

Nomenclature

a_p = particle radius
$\mathscr{B}_m$ = mass transfer driving force
C_f = skin friction coefficient $\equiv 2\tau_s/\rho_e U_e^2$
$\mathscr{D}$ = binary diffusion coefficient
g_m = mass transfer conductance
h = enthalpy
ΔH_r = heat of reaction per lb carbon
j = diffusive mass flux
k = thermal conductivity
M = molecular weight
$\dot{m}''$ = mass transfer rate
m = mass fraction
n = particle number density
p = pressure
Pr = Prandtl number
$\dot{Q}$ = volumetric heat release rate
q = conductive heat flux
Re_θ = Reynolds number based on momentum thickness
$\mathscr{R}$ = universal gas constant
$\dot{r}_1$ = volumetric consumption rate of species 1
Sc = Schmidt number
T = temperature
T^+ = dimensionless temperature $\equiv T/T_e$
u, v = streamwise and normal velocity components, respectively
u^+ = u/v^*
v^* = friction velocity $= (\tau_s/\rho_e)^{1/2}$
$V_{p,\infty}$ = particle velocity relative to vehicle, upstream of shock
x, y = streamwise and normal coordinates, respectively
y^+ = yv^*/v_e
γ_p = particle specific weight
δ = boundary-layer thickness
δ_p = particle boundary-layer thickness
ε^+ = dimensionless total viscosity
κ = von Kármán's constant
μ, ν = dynamic and kinematic viscosity, respectively
$\Omega_{\mathscr{D}}$ = collision integral
ρ = gas density
$\rho_{p,\infty}$ = particle density upstream of shock
σ = collision cross section
τ = shear stress
ϕ = ratio of ejected to incident mass

Subscripts
e = freestream
eff = effective (laminar + turbulent)
p = particle
r = recovery
s = gas phase adjacent to surface
t = transferred state; turbulent
u = heat shield adjacent to surface
1 = oxygen
2 = nitrogen

Received June 10, 1974; revision received August 26, 1974. This work was performed for SAMSO under Air Force Contract F04701-73-C-0095 in support of the Natural Hazards Assessment Program. The SAMSO project officer was L. J. Hudack. The SAI principal investigator for the SAMSO program was L. E. Dunbar.

Index categories: Material Ablation; Reactive Flows; Boundary Layers and Convective Heat Transfer–Turbulent.

* Staff Scientist.

† Consultant; also Associate Professor, School of Engineering and Applied Science, University of California, Los Angeles, Calif. Member AIAA.

Introduction

DURING re-entry a missile might encounter clouds of dust particles, or of ice crystals and water droplets. Impact of such particles on a graphite or other carbonaceous heat shield causes ejection of small carbon particles which combust as they are swept downstream of the vehicle. Preferential ablation or thermal stress may also cause particulate mass loss. There is at present considerable speculation as to whether the combustion of these particles can appreciably augment the heat transfer to the aft heat shield of the vehicle, and hence require ejecta combustion effects to be included in heat shield ablation calculations and design procedures. The analysis presented here was initiated to resolve this question.

For the model problem, the flowfield is taken as conical and the boundary layer turbulent. The carbon particles are assumed to be spherical, of a single radius a_p and are distributed uniformly across a particle boundary layer of thickness δ_p, which is less than or equal to the hydrodynamic boundary-layer thickness δ, and move with the surrounding fluid. The analytical method chosen is to model the turbulent boundary layer as a Couette flow. Such an approach was used by Rubesin and Pappas[1] and others for calculation of turbulent boundary layers with foreign gas injection, and has been subsequently shown to be a very good approximation for constant pressure turbulent boundary layers.[2] Variation of particle radius with distance along the heat shield is not accounted for. The results of the analysis thus show the effects of ejecta combustion subject to the assumption of local self-similarity. The results for the temperature and concentration profiles and associated integral thickness may also be used in an integral formulation wherein the integral forms of the boundary-layer equations are solved by forward integration along the cone. However, the weakly nonsimilar nature of the problem suggests that little further information can be obtained from solving the integral equations and the considerable effort required is not justified. Alternatively, since a finite difference scheme is used here, it is simple to extend the present analysis to solve the full boundary-layer equations.

Particle Combustion Model

In the temperature regime under consideration (3000–6000°R), diffusion-controlled oxidation of carbon to carbon monoxide may be assumed. Kinetics limitations can be shown to be of no consequence for particle sizes greater than 10^{-1} μ. Negligible oxygen dissociation is assumed so that the carbon combustion rate is given by[3]

$$\dot{m}'' = g_m \mathscr{B}_m \tag{1}$$

$$= (\rho\mathscr{D}/a_p)\ln(1+3/4m_1) \tag{2}$$

where m_1 is the mass fraction of O_2 some distance from the particle, and the mass transfer conductance g_m has been taken as that for a sphere in infinite stagnant surroundings. The conductance model will be most appropriate for the smallest particles which follow the turbulent fluctuations and will underestimate the conductance for larger particles due to their longer persisting initial velocity and their inability to follow turbulent fluctuations. However, it is the smaller particles which are more important owing to their higher combustion rates.

The major uncertainty in the use of Eq. (2) arises in the evaluation of the temperature-dependent $\rho\mathscr{D}$ product; some reference value dependent on the particle, flame, and ambient temperatures is required and no such reference value has been established in the literature. For combustion in ambient air the predictions of Eq. (2) may be compared with those of the more exact analysis of Gerstein and Farr[4], which analysis in turn is similar to the early work of Coffin and Brokaw.[5] Equation (2) becomes

$$\dot{m}''a_p/M_c = (\rho\mathscr{D}/12)\ln(1+\tfrac{3}{4}\times 0.232) = 0.01325\rho\mathscr{D} \tag{3}$$

The $\rho\mathscr{D}$ product will be evaluated with ρ for N_2 and $\mathscr{D}$ for an O_2-N_2 mixture. Using the Lennard-Jones potential model in the Chapman-Enskog kinetic theory of gases we have[6]

$$\rho\mathscr{D} = \left(\frac{PM}{\mathscr{R}T_r}\right)\left\{8.283\times 10^{-7}\,\frac{[T_r^3(1/M_1+1/M_2)]^{1/2}}{\sigma_{12}^2\Omega_{\mathscr{D}}P}\right\}\ \text{lb/ft sec}$$

and using the force constant data from Ref. 6,

$$\rho\mathscr{D} = 6.222\times 10^{-5}\,[T_r(°R)^{1/2}/\Omega_{\mathscr{D}}]\ \text{lb/ft sec} \tag{4}$$

Substituting in Eq. (3)

$$\dot{m}''a_p/M_c = 8.265\times 10^{-8}\,[T_r(°R)^{1/2}/\Omega_{\mathscr{D}}]\ \text{lb mole/ft sec} \tag{5}$$

T_r is the reference temperature for the evaluation of the $\rho\mathscr{D}$ product, and the collision integral $\Omega_{\mathscr{D}}$ is tabulated.[6] Table 1 compares the predictions of Eq. (5) with those of Gerstein and Farr.[4] In order to make this comparison of reference temperature $T_r = \frac{1}{2}\times[T_p+(T_e+2700°R)]$ was assumed based on the calculated flame temperatures of Gerstein and Farr.[4]

It is clear from Table 1 that the simple combustion model described by Eq. (2) is adequate for the present purpose, particularly in view of uncertainties in particle size and shape, and particle number density. It also should be noted that Eq. (2) gives the burning rate in terms of the concentration of O_2 in the immediate surroundings, m_1. Since m_1 varies across the boundary layer in our problem a suitable model should contain m_1 explicitly; the results of the more exact analyses[4,5] are for $m_1 = 0.232$ only, and additional results would have to be generated and correlated if such analyses were to be used here.

The stoichiometry of the reaction $2C+O_2\rightarrow 2CO$ requires 4 lbs O_2 to be consumed per 3 lbs of carbon burnt; hence the rate of oxygen consumption per unit volume of boundary layer gas is

Table 1 Carbon particle burning-rate constants

	$(\dot{m}''a_p/M_c)$ lb mole/ft sec $\times 10^5$	
T_r°R	Eq. (5)	Gerstein and Farr[4]
4000	0.83	0.59
5000	0.94	0.71
6000	1.05	1.18

$$\dot{r}_1 = \dot{R}_1\ln(1+\tfrac{3}{4}m_1) \tag{6}$$

where $\dot{R}_1 \equiv (16/3)\pi a_p\rho\mathscr{D}n$ and n is the number density of the particles. Equation (6) can be linearized to read

$$\dot{r}_1 = \dot{R}_1(\tfrac{3}{4}m_1) \tag{7}$$

which form is used in the numerical computations. Since $\rho\mathscr{D} = \mu/Sc$, we can write

$$\rho\mathscr{D} = \frac{\mu}{Sc} = \frac{\mu_e}{Sc}\left(\frac{\mu}{\mu_e}\right) \simeq \frac{\mu_e}{Sc}\left(\frac{T_r}{T_e}\right)^{0.8}$$

where T_r is the reference temperature discussed previously. Then

$$\dot{R}_1 = \frac{16}{3}\pi a_p\left[\frac{\mu_e}{Sc}\left(\frac{T_r}{T_e}\right)^{0.8}\right]n \tag{8}$$

The corresponding rate at which heat is released per unit volume is

$$\dot{Q} = -\tfrac{3}{4}\dot{r}_1(\Delta H_r)\ \text{Btu/ft}^2\ \text{sec} \tag{9}$$

where ΔH_r is the heat of reaction per lb carbon. The particle density n is related to distance along the cone x as[7]

$$n = \frac{3\rho_{p,\infty}V_{p,\infty}\phi\sin\theta}{8\pi\gamma_p a_p^3\delta_p u_e}x \tag{10}$$

and is derived from a simple mass balance. Note that the heat release because of combustion is inversely proportional to a_p^2.

Boundary-Layer Analysis

Couette-Flow Model

Coordinates x and y are taken parallel and perpendicular to the cone surface; the corresponding velocity components are u and v. This mass conservation equation is

$$d/dy(\rho v) = \dot{r}_{co} - \dot{r}_{o_2} \simeq 0 \tag{11}$$

where we have assumed that the gas produced in the combustion of the particles is negligible compared to the transverse mass flux. Integrating,

$$\rho v = \text{const} = (\rho v)_s \equiv \dot{m}'' \tag{12}$$

The remaining conservation equations for high speed turbulent flow in terms of an eddy diffusivity model of turbulent transport are:

momentum:

$$\dot{m}''\,du/dy = d/dy(\mu_{\text{eff}}\,du/dy) \tag{13}$$

species:

$$\dot{m}''\frac{dm_1}{dy} = \frac{d}{dy}\left(\frac{\mu_{\text{eff}}}{Sc_{\text{eff}}}\frac{dm_1}{dy}\right) - \left(\frac{3}{4}\dot{R}_1\right)m_1 \tag{14}$$

energy:

$$\dot{m}''\frac{dT}{dy} = \frac{d}{dy}\left(\frac{\mu_{\text{eff}}}{Pr_{\text{eff}}}\frac{dT}{dy}\right) + \frac{\mu_{\text{eff}}}{C_p}\left(\frac{du}{dy}\right)^2 - \frac{9\Delta H_r\dot{R}_1 m_1}{16C_p} \tag{15}$$

where $\dot{R}_1$ is given by Eq. (8). The boundary conditions are:

$$y=0:\ u=0;\quad -\rho\mathscr{D}_{12}(dm_1/dy) = m_{1,t}\dot{m}'' = \tfrac{3}{4}\dot{m}'';\quad T=T_s$$

$$y\rightarrow y_e:\ u=u_e;\quad m_1 = m_{1,e} = 0.232;\quad T=T_e \tag{16}$$

Dimensionless forms of the governing equations are obtained in the usual manner, and Eqs. (13–15) become

$$B_f\frac{du^+}{dy^+} = \frac{d}{dy^+}\left(\varepsilon^+\frac{du^+}{dy^+}\right) \tag{17}$$

$$B_f\frac{dm_1}{dy^+} = \frac{d}{dy^+}\left(\varepsilon^+\,Sc_{\text{eff}}^{-1}\frac{dm_1}{dy^+}\right) - R_m m_1 \tag{18}$$

$$B_f\frac{dT^+}{dy^+} = \frac{d}{dy^+}\left(\varepsilon^+\,Pr_{\text{eff}}^{-1}\frac{dT^+}{dy^+}\right) + E^*\varepsilon^+\left(\frac{du^+}{dy^+}\right)^2 + E^*R_q m_1 \tag{19}$$

where

$$B_f = \frac{\dot{m}''}{\rho_e v^*} = \frac{\dot{m}''}{\rho_e u_e(C_f/2)^{1/2}};\qquad E^* = \frac{v^{*2}}{C_p T_e g_c J};$$

$$R_m = \frac{3/4\dot{R}_1\mu_e}{\rho_e^2 v^{*2}};\qquad R_q = \frac{-9/16\Delta H_r\dot{R}_1 v_e^2}{\mu_e v^{*2}C_p T_e}$$

The boundary conditions become

$$y^+ = 0: \; u^+ = 0; \quad dm_1/dy^+ = \tfrac{3}{4}Sc_{\text{eff}}B_f; \quad T^+ = T_s/T_e$$
$$y^+ \to y_e{}^+: \; u^+ = (2/C_f)^{1/2}; \quad m_1 = 0.232; \quad T^+ = 1 \qquad (20)$$

Eddy Viscosity Model

The dimensionless total viscosity is defined as

$$\varepsilon^+ = \mu/\mu_e + \mu_t/\mu_e \qquad (21)$$

For the inner region of the boundary layer we use the Landis-Mills model[8] for μ_t

$$\mu_t = \rho(\kappa y^+)^2\{1-\exp[-(y^+/26)(\exp v_s{}^+)^5]\}^2\,(du/dy) \qquad (22)$$

which is a form of the van Driest model developed to apply when surface mass transfer is present. In dimensionless form Eq. (22) is

$$\frac{\mu_t}{\mu_e} = \frac{\rho}{\rho_e}(\kappa y^+)^2\left\{1-\exp\left[-\frac{y^+}{26}\left(\exp\frac{T_s}{T_e}B_f\right)^5\right]\right\}^2\frac{du^+}{dy^+} \qquad (23)$$

For the outer region we use the model proposed by Simpson[9] with continuity of μ_t imposed where the regions meet,

$$\mu_t = \rho\left\{\frac{\kappa}{4}\delta\left[1-\exp\left(-\frac{4y}{\delta}\right)\right]\right\}^2\frac{du}{dy} \qquad (24)$$

or

$$\frac{\mu_t}{\mu_e} = \frac{\rho}{\rho_e}\frac{\kappa^2}{16}y_e{}^{+2}\left[1-\exp\left(-4\frac{y^+}{y_e{}^+}\right)\right]^2\frac{du^+}{dy^+} \qquad (25)$$

The effective Prandtl and Schmidt numbers are given by

$$Pr_{\text{eff}}{}^{-1} = \left[\left(\frac{\mu}{\mu_e}\right)Pr^{-1} + \left(\varepsilon^+ - \frac{\mu}{\mu_e}\right)Pr_t{}^{-1}\right]\Big/\varepsilon^+ \qquad (26)$$

$$Sc_{\text{eff}}{}^{-1} = \left[\left(\frac{\mu}{\mu_e}\right)Sc^{-1} + \left(\varepsilon^+ - \frac{\mu}{\mu_e}\right)Sc_t{}^{-1}\right]\Big/\varepsilon^+ \qquad (27)$$

Thermophysical Properties

Property data for the air boundary layer used was as follows:

$C_p = 0.243$; $\rho \propto T^{-1}$; $\mu \propto T^{0.8}$

$Pr = 0.70$, $Sc = 0.70$

$Pr_t = 0.90$, $Sc_t = 1.00$, $\kappa = 0.40$ following Ref. 8

Other property data includes

$\gamma_p = 83.6$ lb/ft^3, $\Delta H_r = -3960$ Btu/lb

Numerical Procedure

The general form of Eqs. (17–19) is

$$B_f\frac{d\phi_n}{dy} = \frac{d}{dy}\left[F\phi_n\frac{d\phi_n}{dy}\right] + S_n \qquad (28)$$

where the source term is zero for the momentum equation, is set equal to zero for the species equation by combining $-R_m m_1$ with the diffusion term to ensure numerical stability, and for the energy equation is

$$S = E^*\varepsilon^+(du^+/dy^+)^2 + E^*R_q m_1 \qquad (29)$$

Equation (28) was approximated in finite difference form as

$$B_f\left[\frac{\delta_1}{\delta_{12}}\frac{\phi_{i+1}-\phi_i}{\delta_2} + \frac{\delta_2}{\delta_{12}}\frac{\phi_i-\phi_{i-1}}{\delta_1}\right] =$$
$$\frac{1}{\delta_{12}/2}\left[\left(F\phi_{i+1/2}\frac{\phi_{i+1}-\phi_i}{\delta_2}\right) - \left(F\phi_{i-1/2}\frac{\phi_i-\phi_{i-1}}{\delta_1}\right)\right] + S_i \qquad (30)$$

where $\delta_1 = y_i - y_{i-1}$, $\delta_2 = y_{i+1} - y_i$ and $\delta_{12} = \delta_1 + \delta_2$. Equation (30) was cast in the form

$$\phi_i = A_i\phi_{i+1} + B_i\phi_{i-1} + C_i \qquad i = 2, 3, \ldots, N \qquad (31)$$

which is solved for the ϕ's using an efficient tridiagonal matrix elimination algorithm. The domain is divided into N unequal steps where more node points are stacked near the wall in a logarithmic fashion appropriate to turbulent profiles. The coupled finite difference analogs to the conservation equations are solved in an iterative manner, after an initial guess is established for the dependent variables. Iteration proceeds until the maximum difference between two successive iterates is less than some prescribed value ε, that is

$$|1-\phi^{j+1}/\phi^j| \leqq \varepsilon$$

where j denotes the jth iterate. To avoid convergence problems a relaxation scheme is adopted.

Results and Discussion

Table 2 lists the pertinent parameters values for three altitudes for a typical re-entry trajectory, at a position $x =$ 6.12 ft along a cone of half angle $\theta_c = 9°$. Particle sizes considered were $a_p = \infty$ (no burning) 10, 5, 3, and 1 μ. For Cases 1a, b, and c the particle boundary layer of thickness $\delta_p/\delta = 1$, 0.5 and 0.2, respectively, while for Cases 2 and 3, only $\delta_p/\delta = 1.0$ was calculated. In performing the calculations, results were first obtained for $a_p = \infty$ by adjusting $y_e{}^+$ until the listed value of Re_θ was obtained; $y_e{}^+$ was then held constant while a_p was varied. Numerical accuracy was investigated by varying the number of node points across the boundary layer; the results presented here are for $N = 200$.

Table 2 Parameter values for cases calculated

Case	1a, b, c	2	3
Altitude, kft	36	20	10
P, atm	3.36	4.37	4.37
T_e, °R	1,350	1,138	939
T_s, °R	5,000	5,000	5,000
u_e, fps	18,900	15,314	12,475
$\rho_{p,\infty}$, lb/ft^3 × 10^5	1.25	1.25	1.25
$V_{p,\infty}$, fps	19,137	15,600	12,500
ϕ	10.6	6.73	4.10
$Re_\theta \times 10^{-5}$	2.20	2.90	2.90

Table 3 presents the results for the following quantities of interest: 1) The convective heat flux to the surface,

$$q_s = -k\,dT/dy|_s$$

2) The heat flux to the heat shield,

$$q_u = q_s + j_{1,s}(-\tfrac{3}{4}\Delta H_r)$$

3) The skin friction coefficient,

$$C_f/2 = \tau_s/\rho_e u_e{}^2$$

4) The Reynolds analogy factor for mass

$$R_{afm} = \frac{j_{1,s}}{\rho_e u_e(m_{1,e} - m_{1,s})C_f/2} \qquad (32)$$

5) The Reynolds analogy factor for convective heat transfer,

$$R_{afh,s} = q_s/[\rho_e u_e(h_r - h_s)C_f/2] \qquad (33)$$

6) The Reynolds analogy factors for heat transfer to the heat shield,

$$R_{afh,u} = q_u/[\rho_e u_e(h_r - h_s)C_f/2] \qquad (34)$$

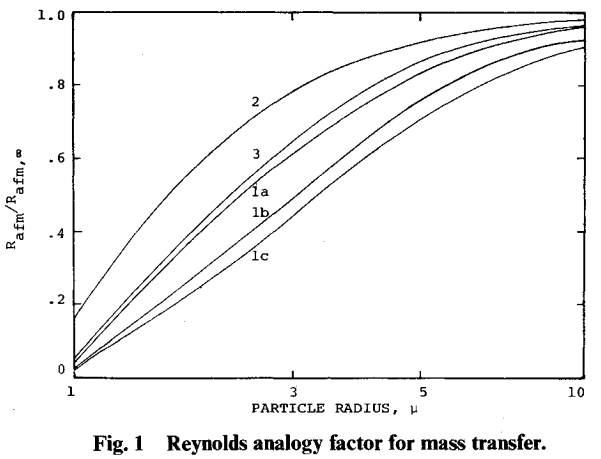

Fig. 1 Reynolds analogy factor for mass transfer.

Table 3 Results of carbon ejecta combustion calculations

Case	Particle radius, μ	q_s Btu/ft^2 sec	q_u Btu/ft^2 sec	$C_f/2\times10^4$	R_{afm}	$R_{afh,s}$	$R_{afh,u}$
1a	∞	2456	2740	2.050	1.063	1.145	1.277
36 Kft	10	2470	2740	2.033	1.017	1.156	1.283
$\delta_p/\delta = 1$	5	2480	2714	2.024	0.883	1.167	1.276
	3	2515	2684	1.989	0.652	1.203	1.285
	1	2559	2569	1.928	0.042	1.263	1.268
1b	10	2496	2761	2.064	0.981	1.151	1.273
36 Kft	5	2528	2742	2.059	0.798	1.168	1.268
$\delta_p/\delta = 0.5$	3	2571	2710	2.038	0.519	1.200	1.265
	1	2627	2633	1.978	0.025	1.265	1.267
1c	10	2483	2742	2.053	0.965	1.151	1.271
36 Kft	5	2539	2741	2.055	0.753	1.176	1.269
$\delta_p/\delta = 0.2$	3	2599	2723	2.044	0.466	1.210	1.268
	1	2690	2696	2.022	0.024	1.266	1.268
2	∞	1926	2299	2.165	1.055	1.143	1.365
20 Kft	10	1932	2295	2.162	1.030	1.148	1.364
$\delta_p/\delta = 1.0$	5	1937	2276	2.138	0.969	1.164	1.368
	3	1956	2242	2.103	0.832	1.196	1.370
	1	2047	2099	1.979	0.161	1.329	1.363
3	∞	1088	1468	2.353	1.055	1.139	1.538
10 Kft	10	1095	1459	2.338	1.015	1.154	1.537
$\delta_p/\delta = 1.0$	5	1118	1436	2.284	0.908	1.206	1.549
	3	1160	1393	2.237	0.679	1.278	1.535
	1	1247	1262	2.039	0.049	1.507	1.526

Reynolds Analogy Factor for Mass Transfer, R_{afm}

Figure 1 shows R_{afm} normalized with the value for no particle combustion $R_{afm,\infty}$. Comparing the curves for Cases 1a, 1b, and 1c it is seen that when the particles are distributed closer to the wall, the amount of oxygen reaching the wall is reduced. The differences in R_{afm} for Cases 1a, 2, and 3 can be explained by comparing values of $R_m = \frac{3}{4}\dot{R}_1\mu_e/\rho_e{}^2v^{*2}$ which is seen in Eq. (18) to scale the oxygen consumption due to particle burning. For example, for $a_p = 1\ \mu$, R_m takes the values 5.96×10^{-6}, 2.47×10^{-6} and 4.93×10^{-6} for Cases 1a, 2, and 3, respectively. Case 2 which has the lowest value of R_m shows the least oxygen depletion in the boundary layer. From the definition of $\dot{R}_1$ it should be noted that $\dot{R}_1$ is proportional to the number of carbon particles ejected into the boundary layer, which in turn is proportional to the product $(\rho_{p,\infty}V_{p,\infty}\phi)$, values of which can be obtained from Table 2.

Skin Friction Coefficient

For Cases 1a, 2, and 3, $C_f/2$ is seen to decrease with decrease of particle size, a trend which can be explained as follows. The skin friction depends essentially on the turbulent viscosity in the law of the wall and outer region of the boundary layer, and Eqs. (22) and (24) show that μ_t is directly proportional to ρ. The increase of heat release in the boundary layer with decreasing particle size causes an increase in T and consequent decrease of ρ and μ_t. This phenomenon is very similar to the well known decrease in skin friction with increase of viscous dissipation heating as the Mach number increases. For Cases 1b and 1c, where the particles are distributed closer to the wall ($\delta_p/\delta = 0.5$ and 0.2, respectively), the temperature in the outer region of the boundary layer is less affected, and thus there is less change in $C_f/2$. The temperature profiles shown in Fig. 2 confirm this behavior.

Convective Heat Flux q_s and Reynolds Analogy Factor, $R_{afh,s}$

The convective heat flux from the boundary layer to the wall, q_s, is seen to increase with decreasing particle size in all the cases (see Fig. 3). In fact there are two opposing trends, 1) an increase of the maximum temperature in the boundary layer, and 2) a decrease in the turbulent conductivity μ_t/Pr_t, with the first effect being dominant. Since $C_f/2$ also decreases because of the decrease in μ_t, the Reynolds analogy factor R_{afh} increases more markedly than q_s. Comparing Cases 1a–c it is seen that as the particles are distributed closer to the wall q_s increases. This trend is both due to the increased temperatures near the wall (see Fig. 2), and to the resulting increase in molecular thermal conductivity ($k \propto T^{0.8}$).

Heat Flux to the Heat Shield q_u, and the Reynolds Analogy Factor $R_{afh,u}$

The results for q_u show that in all cases the net effect of particle ejecta combustion in the boundary layer is to reduce the heat flux into the heat shield (see Fig. 3). One can think of the particles protecting the heat shield by consuming oxygen before it can reach the heat shield and react there; in addition there is the effect of the reduction in the turbulent mass diffusivity μ_t/Sc_t due to increased temperatures in the boundary layer. These two effects outweigh the effect of the increase in temperature potential for heat transfer to the wall. The variable property effect is essentially removed in the normalization with $C_f/2$ to give the Reynolds analogy factor for heat flow into the heat shield, $R_{afh,u}$. Table 3 shows that $R_{afh,u}$ is, for all practical purposes, independent of particle size and distribution, a rather remarkable result in that this invariance results from counteracting factors. Although the molecular Lewis number Pr/Sc was taken as unity, the turbulent Lewis number was taken as 0.9. This nonunity Lewis number effect (which would give an increased q_u for an increase in a_p) is counteracted by the reduction of wall diffusive fluxes due to blowing (which also becomes more significant with increase in a_p). It should, therefore, be noted that the increase in q_u as δ_p/δ is decreased, as shown by Cases 1a–c, is due only to variable property effects.

Engineering Correlation of Results

The fact that $R_{afh,u}$ has proven to be practically independent of particle size and distribution suggests that it would be useful to develop a correlation of $R_{afh,u}$ for $a_p = \infty$. A suitable correlation can be developed directly from the surface energy balance, which reads

$$q_u = q_s + j_{1,s}(-\tfrac{3}{4}\Delta H_r) \tag{35}$$

and can be rearranged as

$$R_{afh,u} = R_{afh,s} + m_{1,e}R_{afm}[(-\tfrac{3}{4}\Delta H_r)/(h_r - h_s)] \tag{36}$$

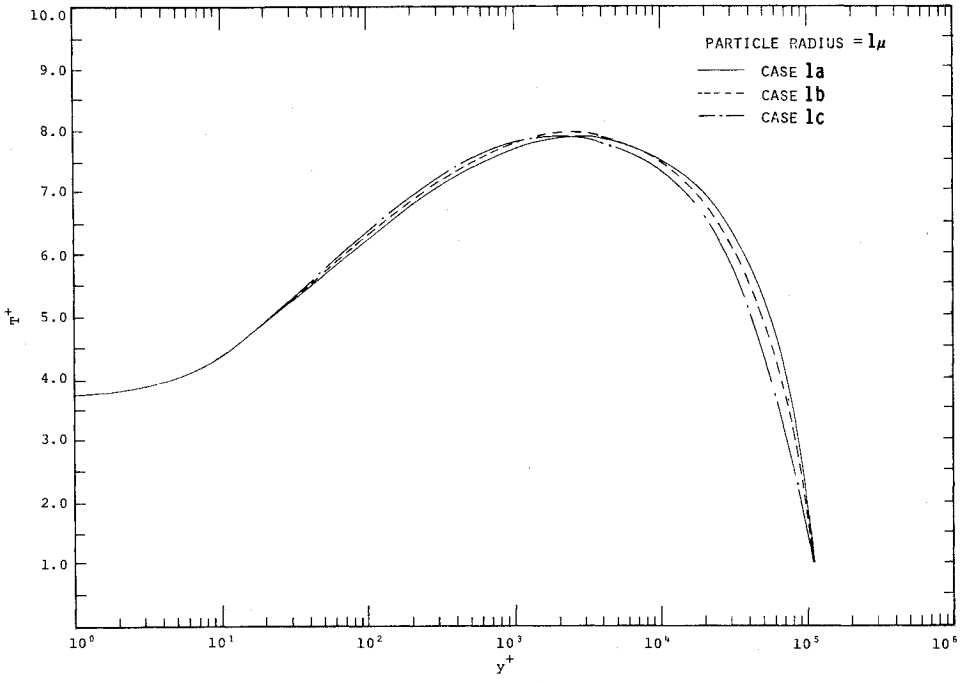

Fig. 2 Dimensionless temperature profiles.

$R_{afh,s}$ can be seen in Table 3 to be approximately 1.14 for all cases calculated, a value which is close to 1.16 which is commonly assumed to hold for supersonic air turbulent boundary layers. R_{afm} for $a_p = \infty$ is seen to be approximately 1.06 for the cases calculated. Then with $m_{1,e} = 0.232$ and $(-\Delta H_r) = 3960$ Btu/lb, Eq. (36) becomes

$$R_{afh,u} = 1.14 + [735/(h_r - h_s)] \tag{37}$$

When the particles are distributed very close to the wall, Eq. (37) can be used in conjunction with a conventional compressible turbulent boundary layer skin-friction calculation to give the heat flux into the heat shield, q_u. When the particles are distributed across the boundary layer the reduced values of $C_f/2$ shown in Table 3 must be accounted for.

Skin friction results presented in Table 3 include the effects of blowing which reduce the unblown values by approximately 8%. To a good approximation, the Schultz-Grunow formula,[10] corrected for both property variations and Mach number effects, can be used for predicting the unblown values. That is,

$$C_f/2 = 0.185\,(\log_{10} Re_x)^{-2.58} CF \tag{38}$$

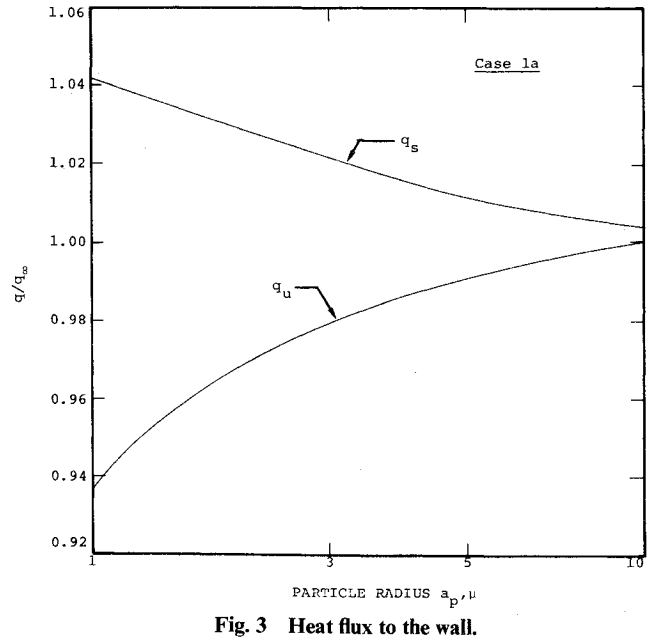

Fig. 3 Heat flux to the wall.

where CF is a correction factor that has the following form

$$CF = (T_r/T_e)^{-0.6}(T_s/T_r)^{-0.4} \tag{39}$$

Properties in Eq. (38) are evaluated at boundary–layer edge temperature.

Conclusions

The effect of carbon particle ejecta burning in the hypersonic turbulent boundary layer on the aft heat shield of a reentry vehicle causes a reduction in the heat flux into the heat shield. The Reynolds analogy factor based on this heat flux is practically independent of particle size and distribution; the reduction in heat flux is due solely to variable property effects caused by increased temperatures in the boundary layer. For engineering purposes the effect of carbon ejecta combustion on aft re-entry vehicle heat shield heat transfer rates may be neglected.

References

[1] Rubesin, M. W. and Pappas, C. C., "An Analysis of the Turbulent Boundary Layer Characteristics on a Flat Plate with Distributed Light Gas Injection," TN 4149, 1958, NACA.

[2] Spalding, D. B., "Contribution to the Theory of Heat Transfer Across a Turbulent Boundary Layer," *International Journal of Heat and Mass Transfer*, Vol. 7, July 1964, pp. 743–762.

[3] Spalding, D. B., *Convective Mass Transfer*, McGraw-Hill, New York, 1963.

[4] Gerstein, M. and Farr, J. L., "Coal Gasification through the Water-Gas Reaction," presented at the Western States Section of the Combustion Institute, Los Angeles, Calif., Oct. 1973.

[5] Coffin, K. P. and Brokaw, R. S., "A General System for Calculating Burning Rates of Particles and Drops and Comparison of Calculated Rates for Carbon, Boron, Magnesium, and Isooctane," TN 3929, 1957, NACA.

[6] Edwards, D. K., Denny, V. E., and Mills, A. F., *Transfer Processes*, Holt, Rinehart and Winston, New York, 1973.

[7] Dunbar, L. E., et al., "Reentry Vehicle Response to Natural Particulate Environments," SAI-73-548-LA, Aug. 15, 1973, Science Applications, Inc., El Segundo, Calif.

[8] Landis, R. B., and Mills, A. F., "The Calculation of Turbulent Boundary Layers with Foreign Gas Injection," *International Journal of Heat and Mass Transfer*, Vol. 15, No. 10, Oct. 1972, pp. 1905–1932.

[9] Simpson, R. L., "Characteristics of Turbulent Boundary Layers at Low Reynolds Numbers With and Without Transpiration," *Journal of Fluid Mechanics*, Vol. 42, July 1970, pp. 769–802.

[10] Kays, W. M., *Convective Heat and Mass Transfer*, McGraw-Hill, New York, 1966.